tained from different sources. Failure was mainly attributed to the very low expression level of gabrb1 protein in the cells and to technical difficulties in distinguishing gabrb1 signals from immunoglobulin heavy chain signals on the blot. Successful detection of endogenous gabrb1 protein in immunoblotting from cultured cells has not been reported.

Gene silencing of other GABAA receptor subunits tested in this study did not affect the PrPres formation in ScN2a cells, suggesting that gabrb1 involvement in the PrPres formation is in a manner irrespective of GABAA receptor. Results from treatments of ScN2a cells with an antagonist picrotoxin and agonists such as GABA, muscimol, pentobarbital, ethanol, and isoguvacine hydrochloride were consistent with this hypothesis. No new function of gabrb1 unrelated to GABAA receptors, except gabrb1 homomeric chloride ion channels, has been reported in the relevant literature. These homomeric channels, expressed in Xenopus oocytes or A293 cells, are sensitive to picrotoxin [22,23], but picrotoxin did not affect the PrPres formation in ScN2a cells. Consequently, gabrb1 function in ScN2a cells might differ from the homomeric channels, which remains to be evaluated.

The gabrb1 gene silencing increased the PrP mRNA level and PrPc protein level. It remains unclear how this happened and whether this resulted from upregulation of PrP gene transcription or from increased stability of PrP mRNA. However, it is noteworthy that the formation of PrPres was reduced despite the increased PrPc expression level. Furthermore, it is noteworthy that treatment with gabrb1 inhibitor, salicylidene salicylhydrazide, decreased the PrPres level but did not modify the PrP expression in either the mRNA level or protein level. The discrepancy between the results of gabrb1 gene silencing and those of gabrb1 inhibitor might reflect the difference in the mRNA/protein expression level of gabrb1: a decreased gabrb1 expression level in the gene silencing versus an unmodified gabrb1 expression level but functional inhibition in the inhibitor. However, further study is necessary to elucidate this speculation.

Compared to ScN2a cells (RML prion-infected N2a cells), N167 cells (22L prion-infected N2a cells) showed less remarkable reduction of PrPres formation in gabrb1 gene silencing. This gap of gabrb1 involvement between ScN2a cells and N167 cells might reflect prion strain difference. Gabrb1 might be more influential in the PrPres formation of RML prion strain, than 22L prion strain. However, we could not exclude possibilities that other factors than prion strain might be responsible for the gap observed between the two cells.

Involvement of GABAergic system in the pathogenesis of prion diseases has been reported [9–15]. The GABAergic neurons are degenerated in an early stage of the disease [13,14]. On the other hand, Trifilo and colleagues [17] report upregulation of GABAA receptor subunits in the prion-inoculated mouse brains expressing anchorless PrP. According to their speculation, inhibitory synaptic transmission is over-stimulated while PrPres formation is promoted; then the inhibitory synaptic transmission system collapses from overwork. Taken together with the findings in this study, suppression of gabrb1 function by inhibitors or other means might be useful for both calming overwhelmed GABAergic systems and inhibiting PrPres formation when conducted at an appropriate stage of the disease.

In conclusion, we identified gabrb1 as a new host factor involved in the PrPres formation in ScN2a cells. Although gabrb1 is a subunit of GABAA receptors, our results suggest that gabrb1 acts on the PrPres formation in a GABAA receptor-independent manner. Because previous literature has not revealed any association of gabrb1 with PrPc [24–30], gabrb1 might function through other cellular factors or directly interact with PrPres as observed in the prion-inoculated mouse brains expressing anchorless PrP [17], where direct association of GABAA receptors with PrPres was demonstrated. The mechanism of gabrb1 involvement in the PrPres formation remains to be elucidated.

Acknowledgements

This study was supported in part by the Program for the Promotion of Fundamental Studies in Health Science of the NIBIO in Japan, and Health and Labour Sciences Research Grants (Research on Intractable Diseases and Research on Food Safety) from the Ministry of Health, Labour, and Welfare of Japan.

Appendix A. Supplementary data

Supplementary data associated with this article can be found, in the online version, at doi:10.1016/j.febslet.2010.02.029.

References

[1] Prusiner, S.B. (1991) Molecular biology of prion diseases. Science 252, 1515–1522.
[2] Gilch, S., Nunziante, M., Ertmer, A. and Schätzl, H.M. (2007) Strategies for eliminating PrP(c) as substrate for prion conversion and for enhancing PrP(Sc) degradation. Vet. Microbiol. 123, 377–386.
[3] Chakrabarti, O., Ashok, A. and Hegde, R.S. (2009) Prion protein biosynthesis and its emerging role in neurodegeneration. Trends Biochem. Sci. 34, 287–295.
[4] Telling, G.C., Scott, M., Mastrianni, J., Gabizon, R., Torchia, M., Cohen, F.E., DeArmond, S.J. and Prusiner, S.B. (1995) Prion propagation in mice expressing human and chimeric PrP transgenes implicates the interaction of cellular PrP with another protein. Cell 83, 79–90.
[5] Kaneko, K., Zulianello, L., Scott, M., Cooper, C.M., Wallace, A.C., James, T.L., Cohen, F.E. and Prusiner, S.B. (1997) Evidence for protein X binding to a discontinuous epitope on the cellular prion protein during scrapie prion propagation. Proc. Natl. Acad. Sci. USA 94, 10069–10074.
[6] Caplen, N.J., Parrish, S., Imani, F., Fire, A. and Morgan, R.A. (2001) Specific inhibition of gene expression by small double-stranded RNAs in invertebrate and vertebrate systems. Proc. Natl. Acad. Sci. USA 98, 9742–9747.
[7] Sui, G., Soohoo, C., Affarel, B., Gay, F., Shi, Y., Forrester, W.C. and Shi, Y. (2002) A DNA vector-based RNAi technology to suppress gene expression in mammalian cells. Proc. Natl. Acad. Sci. USA 99, 5515–5520.
[8] Macdonald, R.L. and Olsen, R.W. (1994) GABAA receptor channels. Annu. Rev. Neurosci. 17, 569–602.
[9] Pocchiari, M., Masullo, C., Lust, W.D., Gibbs Jr., C.J. and Gajdusek, D.C. (1985) Isonicotinic hydrazide causes seizures in scrapie-infected hamsters with shorter latency than in control animals: a possible GABAergic defect. Brain Res. 326, 117–123.
[10] Ferrer, I., Casas, R. and Rivera, R. (1993) Parvalbumin-immunoreactive cortical neurons in Creutzfeldt–Jakob disease. Ann. Neurol. 34, 864–866.
[11] Jefferys, J.G., Empson, R.M., Whittington, M.A. and Prusiner, S.B. (1994) Scrapie infection of transgenic mice leads to network and intrinsic dysfunction of cortical and hippocampal neurones. Neurobiol. Dis. 1, 25–30.
[12] Guentchev, M., Hainfellner, J.A., Trabattoni, G.R. and Budka, H. (1997) Distribution of parvalbumin-immunoreactive neurons in brain correlates with hippocampal and temporal cortical pathology in Creutzfeldt–Jakob disease. J. Neuropathol. Exp. Neurol. 56, 1119–1124.
[13] Guentchev, M., Groschup, M.H., Kordek, R., Liberski, P.P. and Budka, H. (1998) Severe, early and selective loss of a subpopulation of GABAergic inhibitory neurons in experimental transmissible spongiform encephalopathies. Brain Pathol. 8, 615–623.
[14] Belichenko, P.V., Miklossy, J., Belser, B., Budka, H. and Celio, M.R. (1999) Early destruction of the extracellular matrix around parvalbumin-immunoreactive interneurons in Creutzfeldt–Jakob disease. Neurobiol. Dis. 6, 269–279.
[15] Bouzamondo-Bernstein, E., Hopkins, S.D., Spilman, P., Uyehara-Lock, J., Deering, C., Safar, J., Prusiner, S.B., Ralston 3rd, H.J. and DeArmond, S.J. (2004) The neurodegeneration sequence in prion diseases: evidence from functional, morphological and ultrastructural studies of the GABAergic system. J. Neuropathol. Exp. Neurol. 63, 882–899.
[16] Lowry, O.H., Rosebrough, N.J., Farr, A.L. and Randall, R.J. (1951) Protein measurement with the Folin phenol reagent. J. Biol. Chem. 193, 265–275.
[17] Trifilo, M.J., Sanchez-Alavez, M., Solforosi, L., Bernard-Trifilo, J., Kunz, S., McGavern, D. and Oldstone, M.B. (2008) Scrapie-induced defects in learning and memory of transgenic mice expressing anchorless prion protein are associated with alterations in the γ aminobutyric acid-ergic pathway. J. Virol. 82, 9890–9899.
[18] Essrich, C., Lorez, M., Benson, J.A., Fritschy, J.M. and Lüscher, B. (1998) Postsynaptic clustering of major GABAA receptor subtypes requires the γ 2 subunit and gephyrin. Nat. Neurosci. 1, 563–571.
[19] Thompson, S.A., Wheat, L., Brown, N.A., Wingrove, P.B., Pillai, G.V., Whiting, P.J., Adkins, C., Woodward, C.H., Smith, A.J., Simpson, P.B., Collins, I. and Wafford, K.A. (2004) Salicylidene salicylhydrazide, a selective inhibitor of β 1-containing GABAA receptors. Br. J. Pharmacol. 142, 97–106.

[20] Weiner, J.L. and Valenzuela, C.F. (2006) Ethanol modulation of GABAergic transmission: the view from the slice. Pharmacol. Ther. 111, 533–554.
[21] Ashworth-Preece, M., Krstew, E., Jarrott, B. and Lawrence, A.J. (1997) Functional GABAA receptors on rat vagal afferent neurones. Br. J. Pharmacol. 120, 469–475.
[22] Krishek, B.J., Moss, S.J. and Smart, T.G. (1996) Homomeric β 1 γ-aminobutyric acid A receptor-ion channels: evaluation of pharmacological and physiological properties. Mol. Pharmacol. 49, 494–504.
[23] Sanna, E., Garau, F. and Harris, R.A. (1995) Novel properties of homomeric β 1 γ-aminobutyric acid type A receptors: actions of the anesthetics propofol and pentobarbital. Mol. Pharmacol. 47, 213–217.
[24] Lee, K.S., Linden, R., Prado, M.A., Brentani, R.R. and Martins, V.R. (2003) Towards cellular receptors for prions. Rev. Med. Virol. 13, 399–408.
[25] Schmitt-Ulms, G., Hansen, K., Liu, J., Cowdrey, C., Yang, J., DeArmond, S.J., Cohen, F.E., Prusiner, S.B. and Baldwin, M.A. (2004) Time-controlled transcardiac perfusion cross-linking for the study of protein interactions in complex tissues. Nat. Biotechnol. 22, 724–731.
[26] Strom, A., Diecke, S., Hunsmann, G. and Stuke, A.W. (2006) Identification of prion protein binding proteins by combined use of far-Western immunoblotting, two-dimensional gel electrophoresis and mass spectrometry. Proteomics 6, 26–34.
[27] Petrakis, S. and Sklaviadis, T. (2006) Identification of proteins with high affinity for refolded and native PrP^C. Proteomics 6, 6476–6484.
[28] Satoh, J., Obayashi, S., Misawa, T., Sumiyoshi, K., Oosumi, K. and Tabunoki, H. (2009) Protein microarray analysis identifies human cellular prion protein interactors. Neuropathol. Appl. Neurobiol. 35, 16–35.
[29] Rutishauser, D., Mertz, K.D., Moos, R., Brunner, E., Rülicke, T., Calella, A.M. and Aguzzi, A. (2009) The comprehensive native interactome of a fully functional tagged prion protein. PLoS One 4, e4446.
[30] Watts, J.C., Huo, H., Bai, Y., Ehsani, S., Won, A.H., Shi, T., Daude, N., Lau, A., Young, R., Xu, L., Carlson, G.A., Williams, D., Westaway, D. and Schmitt-Ulms, G. (2009) Interactome analyses identify ties of PrP and its mammalian paralogs to oligomannosidic N-glycans and endoplasmic reticulum-derived chaperones. PLoS Pathog. 5, e1000608.

Biochemical and Biophysical Research Communications xxx (2011) xxx–xxx

Contents lists available at ScienceDirect

Biochemical and Biophysical Research Communications

journal homepage: www.elsevier.com/locate/ybbrc

Anti-prion activity of protein-bound polysaccharide K in prion-infected cells and animals

Taichi Hamanaka [a], Yuji Sakasegawa [a], Akihiro Ohmoto [a], Tomohiro Kimura [a], Takao Ando [b], Katsumi Doh-ura [a,*]

[a] Department of Neurochemistry, Tohoku University Graduate School of Medicine, 2-1 Seiryo-machi, Aoba-ku, Sendai 980-8575, Japan
[b] Biomedical Research Laboratory, Kureha, Co. Ltd., 3-26-2 Hyakunin-cho, Shinjuku-ku, Tokyo 169-8503, Japan

ARTICLE INFO

Article history:
Received 31 December 2010
Available online xxxx

Keywords:
Prion
Prion-infected cells
Protein-bound polysaccharide K
Immunotherapeutic agent

ABSTRACT

Protein-bound polysaccharide K (PSK) is a clinical immunotherapeutic agent that exhibits various biological activities, including anti-tumor and anti-microbial effects. In the present study, we report on the anti-prion activity of PSK. It inhibited the formation of protease-resistant abnormal prion protein in prion-infected cells without any apparent alterations in either the normal prion protein turnover or the autophagic function in the cells. Its anti-prion activity was predominantly composed of the high molecular weight component(s) of the protein portion of PSK. A single subcutaneous dose of PSK slightly but significantly prolonged the survival time of peritoneally prion-infected mice, but PSK-treated mice produced neutralizing antibodies against the anti-prion activity of PSK. These findings suggest that PSK is a new anti-prion substance that may be useful in elucidating the mechanism of prion replication, although the structure of the anti-prion component(s) of PSK requires further evaluation.

1. Introduction

Transmissible spongiform encephalopathies or prion diseases include Creutzfeldt–Jakob disease (CJD), Gerstmann–Sträussler–Scheinker syndrome, and familial fatal insomnia in humans. All of these diseases are fatal and characterized by the accumulation of protease-resistant abnormal prion protein, prion, in the brain and lymphoid tissues. Although the precise mechanism of prion propagation remains uncertain, it is commonly assumed that protease-sensitive normal cellular prion protein (PrPc) is converted into protease-resistant abnormal prion protein (PrPres) by direct interaction of the two isoforms [1].

As the occurrences of variant CJD and iatrogenic forms of CJD increase, various efforts to find effective anti-prion remedies have been reported [2]. However, thus far, only a few of anti-prion compounds have been utilized in patients with prion diseases on a trial basis and have reportedly failed to halt the disease progression [3,4]. In these efforts, clinical drugs have been screened for anti-prion activity because they can quickly be brought onstream to be applied to patients with prion diseases [5,6]. We previously tested drugs clinically used in Japan and found one immunotherapeutic agent with anti-prion activity.

Here, we report on the anti-prion activity of the immunotherapeutic agent, protein-bound polysaccharide K (PSK), in prion infected cells and animals, and we discuss the mechanism of its prion-inhibitory activity. PSK is known to be effective in conjunction with chemotherapy and/or radiotherapy for some types of cancers through various immunological modulations [7], and also has anti-microbial activities [8], but this is the first time that its anti-prion activity has been revealed.

2. Materials and methods

2.1. Psk and other immunotherapeutic agents

PSK, a protein-bound polysaccharide preparation extracted from *Coriolus versicolor* with hot water, containing 30% protein and 70% sugar, was obtained from Kureha Co., Ltd. (Tokyo, Japan). The sugar portion is mainly composed of glucans with β-1,4 bonds in the main chain and β-1,3 or β-1,6 bonds in the side chain; the latter binds to the protein portion through O- or N-glycosidic bonds [9]. The protein predominant preparation of PSK (PSK-Pro; 87% protein and 13% sugar) and the sugar predominant preparation of PSK (PSK-Sug; 5% protein and 95% sugar) were also obtained from Kureha. They were prepared by chemical modification of PSK as described previously [10]. Other immunotherapeutic agents clinically utilized in Japan (Lentinan, Schizophyllan, Ubenimex, and Picibanil) were also obtained from their respective pharmaceutical companies. All samples were dissolved in sterile distilled water and stored at 4 °C until use.

* Corresponding author. Fax: +81 22 717 7656.
E-mail address: doh-ura@med.tohoku.ac.jp (K. Doh-ura).

0006-291X/$ - see front matter © 2011 Elsevier Inc. All rights reserved.
doi:10.1016/j.bbrc.2011.01.030

Please cite this article in press as: T. Hamanaka et al., Anti-prion activity of protein-bound polysaccharide K in prion-infected cells and animals, Biochem. Biophys. Res. Commun. (2011), doi:10.1016/j.bbrc.2011.01.030

2.2. Cells and PrP analyses

We used mouse neuroblastoma cells that were either uninfected (N2a cells) or persistently infected with RML scrapie prion (ScN2a cells), 22L prion (N167 cells), or Fukuoka-1 prion (F3 cells), as described previously [11,12]. These cells were cultured in the presence or absence of test samples at 37 °C for 3 days, and confluently grown cells were lysed with lysis buffer. For analysis of PrPres, cell lysate was treated with 10 mg/mL proteinase K at 37 °C for 30 min, and PrPres was precipitated by centrifugation and suspended in a sample loading buffer. For the analysis of other proteins, cell lysate was used without protease treatments and mixed with a concentrated loading buffer. Immunoblotting analysis was performed using standard methods as previously described [11] with an anti-PrP monoclonal antibody (MAb) SAF83 (1:5000), anti-GAPDH MAb (1:5000), anti-β-actin MAb (1:1000), or anti-LC3 MAb (1:2000; nanoTools), followed by alkaline phosphatase-conjugated anti-mouse antibody (1:20,000; Promega). Immunoreactive signals were detected using CDP-Star detection reagent (GE Healthcare). Flow cytometric analysis and floatation assays were also performed to examine PrPc expression in the cells as described previously [11,13].

2.3. Fractionation of PSK constituents

Fractionation of PSK-Pro constituents by gel filtration method was performed in 10 mg of PSK-Pro dissolved in 1 mL of elution buffer (20 mM Tris–HCl, pH 7.5 containing 500 mM NaCl). After ultracentrifugation at 100,000*g* at 4 °C for 30 min, the supernatant was applied to an equilibrated column (1.6 cm diameter and 100 cm length) packed with Sephacryl S-200 HR (GE Healthcare) and eluted with elution buffer. Each fraction containing 6 mL eluate was collected.

2.4. Animal studies

Eight- to ten-week-old Tga20 mice overexpressing murine PrPc [14] were used to analyze the effectiveness of PSK and other immunotherapeutic agents *in vivo*. On the day following a single subcutaneous administration of the maximum tolerated dose of each drug or of vehicle alone, the mice were intraperitoneally infected with 100 μL of 1% (wt/vol) brain homogenate of RML prion. The duration from the infection to the terminal stage of the disease was measured as survival time.

To analyze the anti-PSK neutralizing factors in PSK-dosed mice, sera were collected from the mice 1 month after a single subcutaneous dose of 100 mg PSK or vehicle alone. After clarification of the sera by ammonium sulfate precipitation, IgG fractions were obtained using a protein G column (GE Healthcare). The animal experiments described here were performed with the approval of the Animal Experiment Ethical Committee of Tohoku University.

2.5. Statistical analysis

Data were evaluated using nonparametric Mann–Whitney or Kruskal–Wallis test in the subcutaneous PSK-dosing experiment or the oral multiple PSK-dosing experiment, respectively. Differences were considered significant for p values <0.05.

3. 3. Results

3.1. PSK effects in prion-infected cells

To analyze the inhibitory activity of PSK against PrPres formation in prion-infected cell models, we analyzed PrPres levels in three types of persistently prion-infected cell lines treated with PSK for 3 days. We found that PSK reduced the PrPres levels of all the cells in a dose-dependent manner (Fig. 1A). The 50% effective concentration value (EC_{50}) for PSK in ScN2a cells, N167 cells, and F3 cells was 7.68 μg/mL, 14.45 μg/mL, and 19.01 μg/mL, respectively. Four other clinically used immunotherapeutic agents (Lentinan, Schizophyllan, Ubenimex, and Picibanil) were also tested in ScN2a cells, which are the most sensitive to screening for anti-prion activities [11,12]. However, these four drugs did not exhibit the inhibitory activity against PrPres formation even when tested at maximum tolerated doses (data not shown).

To determine the efficacy of PSK, ScN2a cells were treated with 20 μg/mL PSK for 7 days, and subsequently the cells were cultured in the absence of PSK for a further 27 days. The results showed that PrPres levels did not recover to the detection limit of immunoblotting, suggesting irreversible inhibition of PrPres formation by PSK (Supplementary Fig. 1A). On the other hand, the postseeding 48 h treatment of ScN2a cells with 20 μg/mL PSK reduced the PrPres level to almost the same level (approximately 37% of the untreated ScN2a cells) as the 72 h treatment, while the postseeding 24 h treatment reduced only about 43% of the untreated ScN2a cells (Fig. 1B). This indicates that the inhibition of PrPres formation by PSK is dependent on the treatment duration to some extent. We also examined the direct effects of PSK on PrPres in the cell lysate. Incubation of ScN2a cell lysate with PSK before or after proteinase K treatment did not alter the PrPres levels (Supplementary Fig. 1B). This suggests that PSK does not either degrade PrPres directly or make PrPres protease-sensitive.

3.2. PSK influence on PrPc profiles and autophagy

Because alterations of the PrPc turnover in the cells cause modification of PrPres levels, we analyzed the PrPc levels in N2a cells treated with PSK. Total PrPc and cell surface PrPc levels were not apparently affected by PSK (Fig. 2A and B). Next, we examined the distribution of PrPc in the lipid raft microdomain by floating assay (Fig. 2C), and no significant difference was observed between PSK-treated and untreated cells. These results suggest that PSK does not modify the PrPc turnover.

Because it has been reported that the induction of cellular autophagy facilitates the clearance of aggregate-prone proteins [15], we analyzed the expression levels of LC3-II, an autophagosome formation marker, in PSK-treated ScN2a cells. As shown in Fig. 2D, LC3-II expression levels were not altered in the PSK-treated cells, while treatment of the cells with trehalose, which is known to induce cellular autophagy, caused both a decrease in PrPres levels and an increase in LC3-II expression levels, as reported previously [16]. This indicates that the PSK anti-prion activity is not related to autophagy induction.

3.3. PSK effects in prion-infected mice

We next addressed whether PSK could prolong the survival time of prion-infected mice. This was investigated by intraperitoneally inoculating Tga20 mice with RML prion strain, followed by a single subcutaneous administration of 100 mg PSK. PSK showed slight but significant prolongation of survival period in intraperitoneally infected mice in two independent experiments (128 ± 17.1 days in PSK ($n = 6$) versus 110 ± 3.8 days in control ($n = 6$) in experiment 1 ($p < 0.05$); 100 ± 6.1 days in PSK ($n = 5$) versus 93 ± 2.2 days in control ($n = 5$) in experiment 2 ($p < 0.05$)). However, when PSK was administered orally *ad libitum*, from intraperitoneal infection to disease terminal, mixed with feed at the following doses: 1%, 2%, and 4% with weight in the feed corresponding, respectively to *ca.* 1.5, *ca.* 3.0, and *ca.* 6.0 g/kg body weight/day, and no significant prolongation of survival period was observed

Please cite this article in press as: T. Hamanaka et al., Anti-prion activity of protein-bound polysaccharide K in prion-infected cells and animals, Biochem. Biophys. Res. Commun. (2011), doi:10.1016/j.bbrc.2011.01.030

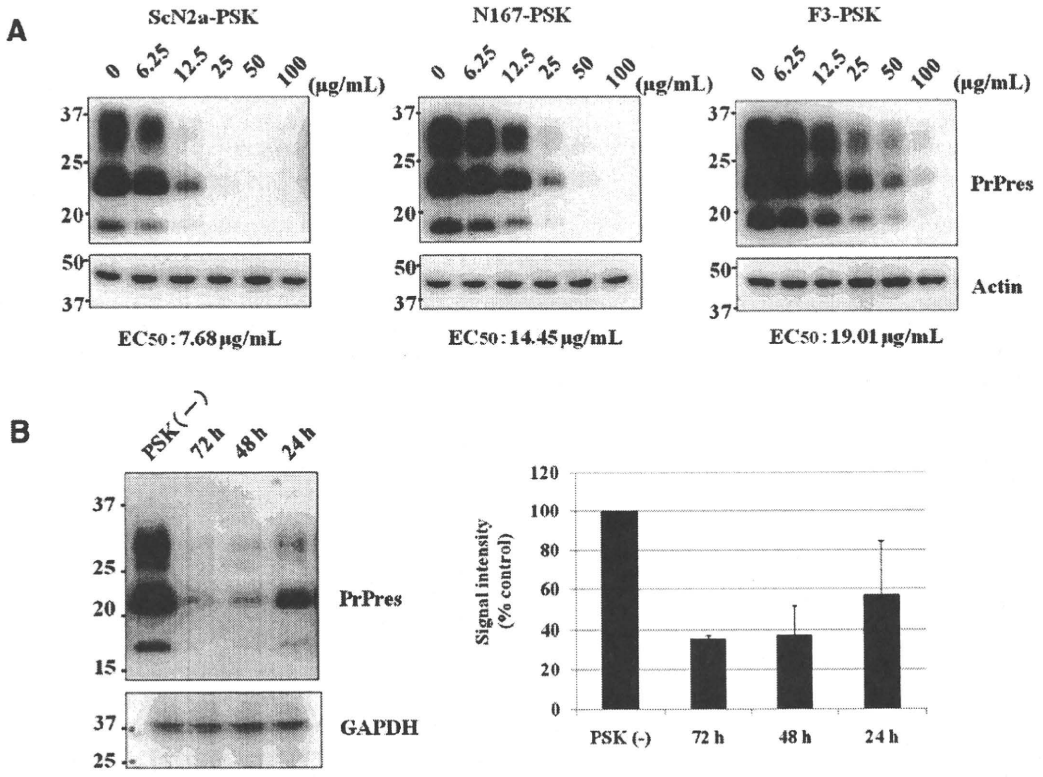

Fig. 1. Inhibitory effects of PSK on PrPres formation in various prion-infected cell models. (A) Each model of persistently prion-infected cells was treated with the indicated concentration of PSK for 3 days, and the PrPres levels were analyzed by immunoblotting. Molecular size markers on the left side of the immunoblots are shown in kilodaltons. (B) Incubation duration-dependent effects of PSK on the PrPres levels were examined by treating ScN2a cells with 20 μg/mL of PSK for 24, 48, or 72 h prior to the harvest.

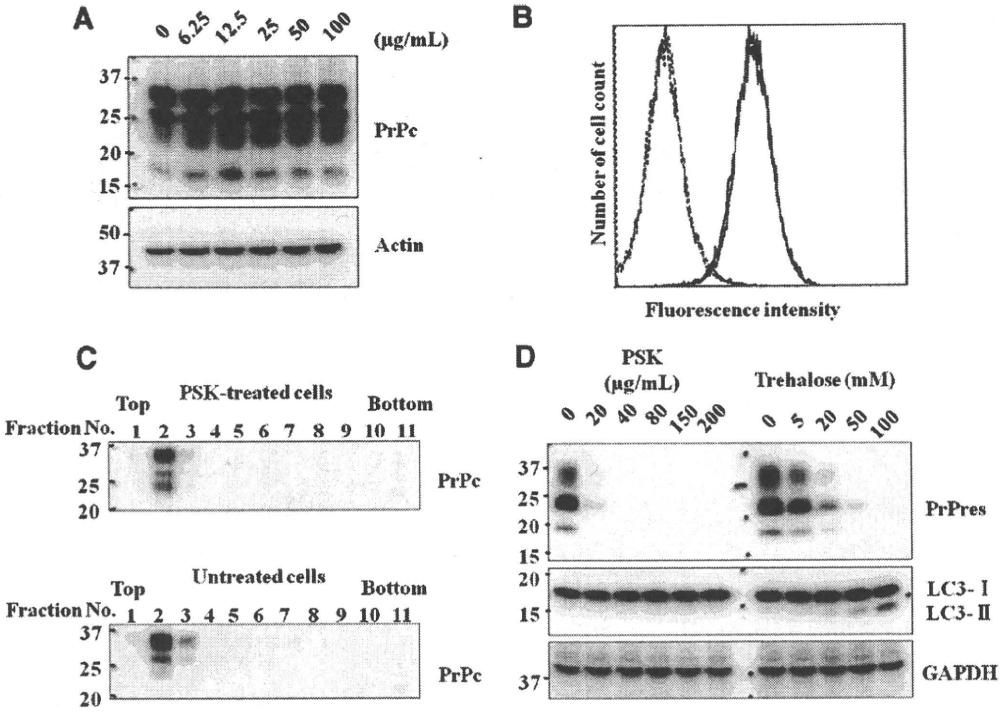

Fig. 2. No apparent effects of PSK on the turnover of PrPc and cellular autophagy. (A) Immunoblot analysis of total PrPc was performed in noninfected N2a cells treated with the indicated concentration of PSK for 3 days. (B) Flow cytometric analysis of PrPc on the cell surface was performed in noninfected N2a cells treated with 20 μg/mL of PSK for 3 days. Gray and black lines indicate PSK-treated cells and untreated cells, respectively. The broken line peaks on the left show their respective isotype controls. (C) Analysis of the distribution of PrPc in the lipid raft was performed by floatation assay in noninfected N2a cells treated with or without 20 μg/mL of PSK. (D) Involvement of autophagy induction was examined in ScN2a cells treated with the indicated concentration of PSK or trehalose for 3 days. Trehalose was used as a positive control of autophagy induction. Both LC3-II and PrPres levels were analyzed by immunoblotting.

Please cite this article in press as: T. Hamanaka et al., Anti-prion activity of protein-bound polysaccharide K in prion-infected cells and animals, Biochem. Biophys. Res. Commun. (2011), doi:10.1016/j.bbrc.2011.01.030

(data not shown). These results suggest that PSK is ineffective in prolonging survival period in prion-infected mice when orally administered, as is normal in clinical situations.

We also similarly tested other immunotherapeutic agents in intraperitoneally prion-infected Tga20 mice. No significant prolongation of survival period was observed, even at the maximum tolerated doses (data not shown).

3.4. Anti-prion components in PSK

We tried to separate anti-prion active components in PSK by using polyacrylamide gel electrophoreses, such as SDS–PAGE, DOC–PAGE, and native PAGE, but PSK constituents were not successfully separated as distinct bands, even after PSK was dissolved in 8 M urea or 6 M guanidine hydrochloride (data not shown). However, the anti-prion activity of PSK was reduced when PSK was treated with a protease and/or a protein denaturant (Fig. 3A). Then, we tried to determine whether anti-prion components in PSK were in the PSK-Pro portion (sugar:protein = 13:87) or the PSK-Sug portion (sugar:protein = 95:5). As shown in Fig. 3B, the prominent anti-prion activity was observed in PSK-Pro. Its EC_{50} value was 3.14 μg/mL, although that of PSK-Sug was more than 50 μg/mL. To further study the active components of PSK-Pro, we analyzed PSK-Pro using Sephacryl S-200 HR gel filtration chromatography. PSK-Pro showed a single sharp peak around 150 kDa, estimated with silver staining after SDS–PAGE, which was eluted in Fraction-2 (Supplementary Fig. 1C, Fig. 3C). This high molecular weight fraction sample of PSK-Pro had strong inhibitory activity against the PrPres formation in ScN2a cells (Fig. 3D). The results indicate that a *ca.* 150 kDa-sized protein-related substance contains the main anti-prion component(s) of PSK.

3.5. Anti-PSK neutralizing antibody in PSK-injected mice

We speculated why the effect on survival periods in PSK-injected mice was not pronounced. Then, from the findings described above, we presumed that the mice injected with PSK could produce antibodies against PSK constituents that antagonize the anti-prion activity of PSK. To examine this inference, IgG fractions were obtained from the Tga20 mice 1 month after a single subcutaneous injection of 100 mg of PSK. After PSK was incubated with purified IgG fractions at 37 °C for 3 h, its anti-prion activity was tested in ScN2a cells. The IgG fractions purified from PSK-injected mice showed neutralizing activity against PSK, but those from untreated control mice did not (Fig. 4). This result suggests that the effects of PSK in mice might be antagonized by anti-PSK neutralizing antibodies produced in PSK-injected mice.

4. Discussion

In this study we revealed that PSK, a clinically used immunotherapeutic agent, is effective in inhibiting the PrPres formation in cell models of persistent prion infection as well as prolonging the survival period of prion-infected animals. The precise mechanism of the PrPres formation is still enigmatic, but it is assumed that PrPc molecules, which mainly localize in the lipid raft microdomain of the cell membrane, are altered to PrPres conformers through direct interaction with PrPres molecules [17–19]. Thus far, it has been demonstrated that lactoferrin [20] and some types of anti-PrP monoclonal antibodies [21] inhibit PrPres formation by affecting the PrPc turnover. PSK, however, neither altered the total or cell surface PrPc levels nor modified the localization of PrPc in the lipid raft microdomain. This suggests that the anti-prion

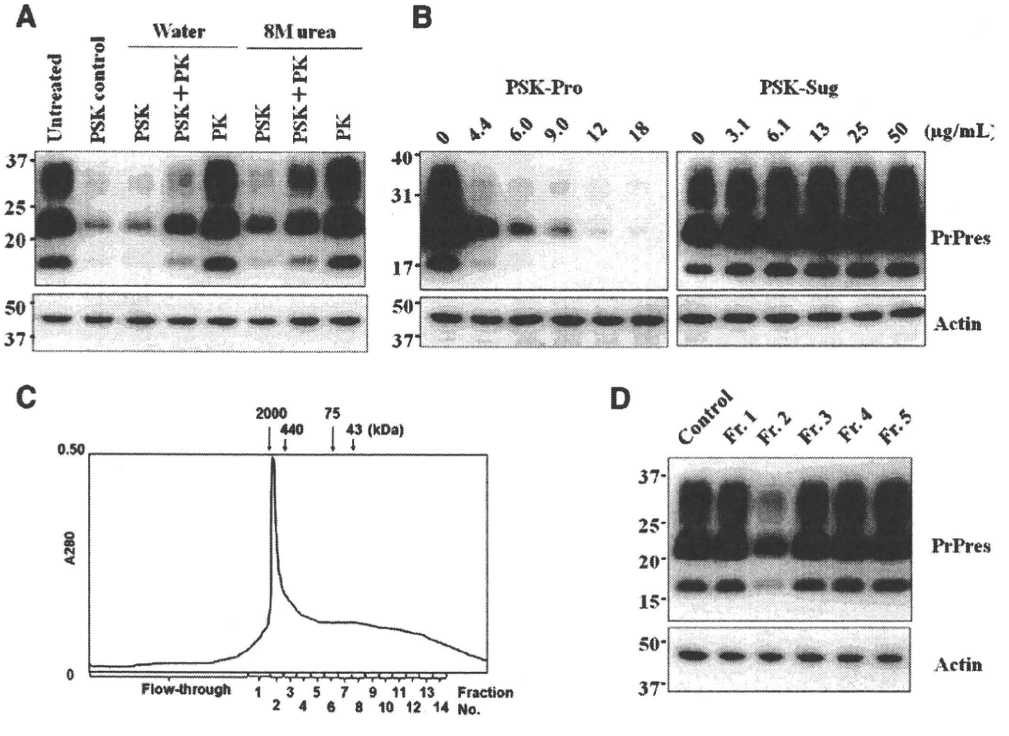

Fig. 3. Effects of PSK-Pro and PSK-Sug on the PrPres formation in ScN2a cells. (A) Immunoblot analysis of PrPres was performed in ScN2a cells treated for 3 days with 20 μg/mL of modified PSK prepared by protease digestion in the presence or absence of protein denaturant as followed. PSK in water or 8 M urea was digested with 700 μg/mL of proteinase K at 37 °C for 7 days and was dialyzed with water after inactivation of the protease by heating at 95 °C for 10 min. PSK control and untreated control in the immunoblot indicate the PrPres samples from the cells treated with freshly prepared 20 μg/mL PSK or vehicle only, respectively. (B) Immunoblot analysis of PrPres was performed in ScN2a cells treated with the indicated concentrations of PSK-Pro or PSK-Sug for 3 days. (C) Gel filtration chromatography of PSK-Pro was performed with Sephacryl S-200HR. Molecular size markers in kilodaltons are shown as arrows on the top of the chromatograph. (D) Anti-prion activities of fractionated PSK-Pro samples were examined by analyzing PrPres levels in ScN2a cells treated with the samples in a concentration of 3.75% in the culture medium for 3 days.

Please cite this article in press as: T. Hamanaka et al., Anti-prion activity of protein-bound polysaccharide K in prion-infected cells and animals, Biochem. Biophys. Res. Commun. (2011), doi:10.1016/j.bbrc.2011.01.030

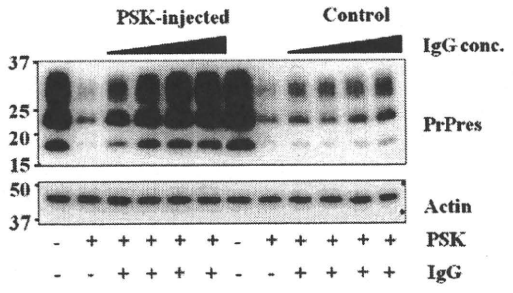

Fig. 4. Anti-PSK activity of IgG purified from PSK-injected mice. Anti-prion activity of PSK in ScN2a cells was neutralized by the addition of IgG purified from PSK-administered mice but not from vehicle-administered control mice. IgG fractions were purified from Tga20 mice subcutaneously administered 100 mg of PSK (PSK-injected) or only vehicle (control). ScN2a cells were treated with 20 μg/mL PSK alone or with a mixture of 20 μg/mL PSK and purified IgG fractions for 3 days.

activity of PSK is not attributable to any apparent alterations in the PrPc turnover of the cells.

On the other hand, cellular autophagy is known to facilitate the clearance of abnormally aggregated proteins [15]. Aguib et al. have reported that either lithium or trehalose enhance the clearance of PrPres molecules in prion-infected cells through the induction of cellular autophagy [16]. The present study, however, suggests that PSK does not enhance this clearance pathway of PrPres molecules, because PSK treatment of prion-infected cells did not induce autophagosome formation. Furthermore, the direct interaction of PrPres molecules with anti-prion compounds such as tetracycline and doxycycline [22] has also been reported to facilitate the degradation of PrPres molecules by protease digestion *in vitro*, but PSK treatment of ScN2a cell lysate before or after protease digestion did not influence the PrPres levels. This indicates that PSK does not have activities that change PrPres molecules into PK-sensitive conformers or proteolytically degrading PrPres molecules. Then, taken together with the findings of the present study in the cell models, it is likely that PSK inhibits the conversion of PrPc to PrPres directly or indirectly through, as yet, unrevealed cellular factors.

PSK is orally administered in combination with other chemotherapeutic agents to cancer patients to enhance their immunity to cancer. The anti-cancer activity of orally administered PSK has been confirmed using some animal models [23]. However, orally administered PSK did not prolong the survival periods of intraperitoneally prion-infected mice in the present study. This suggests that high molecular weight constituents of PSK, which were shown to be responsible for the anti-prion activity in prion-infected cells in the present study, are degraded through the process of absorption from the digestive tract. In fact, it has been reported that almost all of the metabolites of PSK in the urine, feces, and bile of animals orally administered PSK consist of low molecular weight components [24]. On the other hand, subcutaneously administered PSK was effective in prolonging the survival period of prion-infected mice, possibly because it might be absorbed into the circulation through surrounding lymph ducts and microvessels without degradation.

In addition to the discrepancy in the effects of PSK in prion-infected mice between clinically used oral dosing and subcutaneous dosing, three other lines of evidence in the present study suggest that the anti-prion activity of PSK is independent of the primary actions of PSK as an immune system boosting anti-cancer drug. The first is that the anti-prion activity of PSK was mainly present in the high molecular weight protein-related constituents, which are totally different from the main components, polysaccharides, responsible for the actions of not only PSK but also other immunotherapeutic agents, such as Lentinan and Schizophyllan, tested in the present study [23]. The second is that neutralizing IgG antibodies against the anti-prion activity of PSK were produced in the mice that were subcutaneously administered PSK. Although some reports have shown that anti-PSK polyclonal antibodies that can be used to analyze the pharmacokinetics of PSK are produced in immunized rabbits, it has never been reported that antibodies capable of neutralizing the anti-cancer effects of PSK were produced in the mice [25]. In addition, low affinity antibodies are more likely to be produced than high affinity neutralizing antibodies if the antigens are polysaccharides. The third is that other immunotherapeutic agents tested in this study showed no apparent effectiveness in both cell and animal models of prion infection. Therefore, the anti-prion activity of PSK is unlikely to be mediated by activation of innate immunity as previously reported in CpG oligonucleotide [26].

In conclusion, the effectiveness of PSK in both prion-infected cells and prion-infected mice was demonstrated in the present study. It was suggested that PSK exhibits the anti-prion activity through a different mechanism from those already known in its role as an immune system boosting anti-cancer drug. We could not test the effects of PSK-Pro and PSK-Sug in prion-infected animals because of limited test sample availability, but it is evident that PSK is a new type of anti-prion substance that may be useful for elucidating the mechanism of prion replication. However, the structure of anti-prion component(s) of PSK requires further evaluation.

Acknowledgments

We thank Keiko Nishizawa and Ayumi Oguma from Tohoku University for their technical assistance. This study was supported by the Health and Labor Sciences Research Grants (Research on Measures for Intractable Diseases) from the Ministry of Health, Labor, and Welfare of Japan, and by the Program for the Promotion of Fundamental Studies in Health Science of the NIBIO in Japan.

Appendix A. Supplementary data

Supplementary data associated with this article can be found, in the online version, at doi:10.1016/j.bbrc.2011.01.030.

References

[1] S.B. Prusiner, Molecular biology of prion diseases, Science 252 (1991) 1515–1522.
[2] V.L. Sim, B. Caughey, Recent advances in prion chemotherapeutics, Infect. Disord. Drug Targets 9 (2009) 81–91.
[3] J. Collinge, M. Gorham, F. Hudson, A. Kennedy, G. Keogh, S. Pal, M. Rossor, P. Rudge, D. Siddique, M. Spyer, D. Thomas, S. Walker, T. Webb, S. Wroe, J. Darbyshire, Safety and efficacy of quinacrine in human prion disease (PRION-1 study): a patient-preference trial, Lancet Neurol. 8 (2009) 334–344.
[4] Y. Tsuboi, K. Doh-Ura, T. Yamada, Continuous intraventricular infusion of pentosan polysulfate: clinical trial against prion diseases, Neuropathology 29 (2009) 632–636.
[5] D.A. Kocisko, G.S. Baron, R. Rubenstein, J. Chen, S. Kuizon, B. Caughey, New inhibitors of scrapie-associated prion protein formation in a library of 2000 drugs and natural products, J. Virol. 77 (2003) 10288–10294.
[6] C. Korth, B.C. May, F.E. Cohen, S.B. Prusiner, Acridine and phenothiazine derivatives as pharmacotherapeutics for prion disease, Proc. Natl. Acad. Sci. USA 98 (2001) 9836–9841.
[7] H. Kobayashi, K. Matsunaga, M. Fujii, PSK as a chemopreventive agent, Cancer Epidemiol. Biomarkers Prev. 2 (1993) 271–276.
[8] H. Harada, H. Sakagami, K. Konno, T. Sato, N. Osawa, M. Fujimaki, N. Komatsu, Antimicrobial activity induction by PSK subfractions: dependence on molecular weight, Infection 17 (1989) 38–39.
[9] S. Tsukagoshi, Y. Hashimoto, Ç. Fujii, H. Kobayashi, K. Nomoto, K. Orita, Krestin (PSK), Cancer Treat. Rev. 11 (1984) 131–155.
[10] Y. Ohmura, K. Matsunaga, I. Motokawa, K. Sakurai, T. Ando, Protective effects of a protein-bound polysaccharide, PSK, on Candida albicans infection in mice via tumor necrosis factor-alpha induction, Int. Immunopharmacol. 1 (2001) 1797–1811.
[11] Y. Kawasaki, K. Kawagoe, C.J. Chen, K. Teruya, Y. Sakasegawa, K. Doh-ura, Orally administered amyloidophilic compound is effective in prolonging the

incubation periods of animals cerebrally infected with prion diseases in a prion strain-dependent manner, J. Virol. 81 (2007) 12889–12898.
[12] K. Ishikawa, K. Doh-ura, Y. Kudo, N. Nishida, I. Murakami-Kubo, Y. Ando, T. Sawada, T. Iwaki, Amyloid imaging probes are useful for detection of prion plaques and treatment of transmissible spongiform encephalopathies, J. Gen. Virol. 85 (2004) 1785–1790.
[13] K. Teruya, K. Nishizawa, K. Doh-ura, Semisynthesis of a protein with cholesterol at the C-terminal, targeted to the cell membrane of live cells, Protein J. 29 (2010) 493–500.
[14] M. Fischer, T. Rülicke, A. Raeber, A. Sailer, M. Moser, B. Oesch, S. Brandner, A. Aguzzi, C. Weissmann, Prion protein (PrP) with amino-proximal deletions restoring susceptibility of PrP knockout mice to scrapie, EMBO J. 15 (1996) 1255–1264.
[15] S. Sarkar, D.C. Rubinsztein, Small molecule enhancers of autophagy for neurodegenerative diseases, Mol. Biosyst. 4 (2008) 895–901.
[16] Y. Aguib, A. Heiseke, S. Gilch, C. Riemer, M. Baier, H.M. Schätzl, A. Ertmer, Autophagy induction by trehalose counteracts cellular prion infection, Autophagy 5 (2009) 361–369.
[17] N. Naslavsky, R. Stein, A. Yanai, G. Friedlander, A. Taraboulos, Characterization of detergent-insoluble complexes containing the cellular prion protein and its scrapie isoforms, J. Biol. Chem. 272 (1997) 6324–6331.
[18] B. Caughey, G.J. Raymond, The scrapie-associated form of PrP is made from a cell surface precursor that is both protease- and phospholipase-sensitive, J. Biol. Chem. 266 (1991) 18217–18223.
[19] M. Vey, S. Pilkuhn, H. Wille, R. Nixon, S.J. DeArmond, E.J. Smart, R.G. Anderson, A. Taraboulos, S.B. Prusiner, Subcellular colocalization of the cellular and scrapie prion proteins in caveolae-like membranous domains, Proc. Natl. Acad. Sci. USA 93 (1996) 14945–14949.
[20] Y. Iwamaru, Y. Shimizu, M. Imamura, Y. Murayama, R. Endo, Y. Tagawa, Y. Ushiki-Kaku, T. Takenouchi, H. Kitani, S. Mohri, T. Yokoyama, H. Okada, Lactoferrin induces cell surface retention of prion protein and inhibits prion accumulation, J. Neurochem. 107 (2008) 636–646.
[21] C.L. Kim, A. Karino, N. Ishiguro, M. Shinagawa, M. Sato, M. Horiuchi, Cell-surface retention of PrPC by anti-PrP antibody prevents protease-resistant PrP formation, J. Gen. Virol. 85 (2004) 3473–3482.
[22] G. Forloni, S. Jussich, T. Awan, L. Colombo, N. Angeretti, L. Girola, I. Bertani, G. Poli, M. Caramelli, M. Grazia Bruzzone, L. Farina, L. Limido, G. Rossi, G. Giaccone, J.W. Ironside, O. Bugiani, M. Salmona, F. Tagliavini, Tetracyclines affect prion infectivity, Proc. Natl. Acad. Sci. USA 99 (2002) 10849–10854.
[23] S.P. Wasser, Medicinal mushrooms as a source of antitumor and immunomodulating polysaccharides, Appl. Microbiol. Biotechnol. 60 (2002) 258–274.
[24] M. Ikuzawa, K. Matsunaga, S. Nishiyama, S. Nakajima, Y. Kobayashi, T. Andoh, A. Kobayashi, M. Ohhara, Y. Ohmura, T. Wada, Y. Chikao, Fate and distribution of an antitumor protein-bound polysaccharide PSK (Krestin), Int. J. Immunopharmacol. 10 (1988) 415–423.
[25] H. Endoh, K. Matsunaga, C. Yoshikumi, Y. Kawai, T. Suzuki, K. Nomoto, Production of antiserum against antitumor protein-bound polysaccharide preparation, PSK (Krestin) and its pharmacological application, Int. J. Immunopharmacol. 10 (1988) 103–109.
[26] S. Sethi, G. Lipford, H. Wagner, H. Kretzschmar, Postexposure prophylaxis against prion disease with a stimulator of innate immunity, Lancet 360 (2002) 229–230.

Please cite this article in press as: T. Hamanaka et al., Anti-prion activity of protein-bound polysaccharide K in prion-infected cells and animals, Biochem. Biophys. Res. Commun. (2011), doi:10.1016/j.bbrc.2011.01.030

Protein J (2010) 29:493–500
DOI 10.1007/s10930-010-9278-9

Semisynthesis of a Protein with Cholesterol at the C-Terminal, Targeted to the Cell Membrane of Live Cells

Kenta Teruya · Keiko Nishizawa · Katsumi Doh-ura

Published online: 3 September 2010

Abstract Various proteins are modified post-translationally to localize them at the cell membrane. Among them, hedgehog-family proteins are modified by cholesterol at the C-terminal. In this study, green fluorescent protein (GFP) modified with cholesterol (GFP-Chol) at the C-terminal was prepared semisynthetically and investigated. This semi-synthesis was performed using the following native chemical ligation: GFP-Cα-thioester was prepared using the intein-mediated thioester exchange reaction and was ligated to Cys-NH-diethylene glycol-NHCO-cholesterol in the presence of a detergent. After removal of the detergent, the GFP-Chol was applied to mouse live cells. Confocal laser fluorescent microscopy confirmed localization of GFP-Chol at the cell membrane. The findings suggest that modifying proteins with cholesterol at the C-terminal is useful for targeting the proteins to the cell membrane of live cells.

Keywords Chemical modification · C-terminal · Cholesterol · Cell membrane · Semi-synthesis

Abbreviations

Chol	Cholesterol
CTAB	Cetyl trimethyl ammonium bromide
DEG	Diethylene glycol
F	Fluorescein
FAB	Fast atom bombardment
GFP	Green fluorescent protein
MALDI-TOF	Matrix-assisted laser desorption ionization-time of flight
MESNa	Mercapto ethane sulfonic acid sodium salt
MS	Mass spectrometry
PBS	Phosphate-buffered saline
PCR	Polymerase chain reaction
RP-HPLC	Reversed phase-high performance liquid chromatography
SDS-PAGE	Sodium dodecyl sulfate-polyacrylamide gel electrophoresis
TLC	Thin layer chromatography

Electronic supplementary material The online version of this article (doi:10.1007/s10930-010-9278-9) contains supplementary material, which is available to authorized users.

K. Teruya · K. Nishizawa · K. Doh-ura (✉)
Department of Neurochemistry, Tohoku University Graduate School of Medicine, 2-1 Seiryo-Machi, Aoba-Ku, Sendai, Miyagi 980-8575, Japan
e-mail: doh-ura@med.tohoku.ac.jp

1 Introduction

Most proteins require post-translational modifications to exert their functions in live cells. Modification of proteins with lipophilic molecules is necessary for targeting them to the cell membrane and for making them functional in signal transductions and cell–cell interactions. Hedgehog-family proteins, for example, exert developmental signal transductions over the cells neighboring the source of the signal [10], once modified with cholesterol at the C-terminal.

Targeting exogenous artificial proteins to the cell membrane can be useful for pursuing their functions and their interaction with other molecules expressed on the cell membrane of live cells. Common techniques for introducing proteins into live cells include gene transfection, protein modification by an attachment of intracellular compartment localization signals, and receptor-mediated

protein transport. However, no technique has been established to introduce exogenous artificial proteins into the cell membranes of live cells.

We describe the development of a semi-synthetic model protein with a lipophilic molecule at the C-terminal. It was integrated into the cell membrane of live culture cells when added to the cells exogenously. The semi-synthetic protein was produced using a combination of peptide chemical synthesis and recombinant protein-Cα thioester modification technique [3]. The building blocks were ligated by the native chemical ligation method [1, 4, 6, 11], in which a peptide bond is formed via a thiol exchange reaction and an S–N acyl shift between the thioester of a peptide segment and the N-terminal Cys-residue of another peptide segment in aqueous solution.

2 Materials and Methods

Experimental procedures and data are provided in detail in *Supplementary Information*.

2.1 Cloning of GFP-Intein-Chitin Binding Domain

A DNA fragment corresponding to green fluorescent protein (GFP) was obtained from pQBI-pkg (Wako Chemicals USA Inc., VA, USA) using PCR with the primers 5′-CCGG ATCCGGGGCGCGCAAGA-3′ and 5′-CCGCTCGAGAC CGTGTACAGTTCATCCA-3′. This fragment was digested with *Nhe*I and *Xho*I and was ligated into pTYB1 (New England Biolabs Inc.). The resulting plasmid, pGFP/TYB1, contained a DNA sequence of a fusion protein for GFP, a five amino acid peptide linker (Leu-Glu-Gly-Ser-Ser), and a *Saccharomyces cerevisiae* intein with an affinity tag, the chitin-binding domain, placed at the C-terminal. Using this plasmid as a template, we prepared an insert for another vector pTXB1 (New England Biolabs Inc.) using PCR with the primers 5′-TAATACGACTCACTATAGGG-3′ and 5′-CTTGCTCTTCGGCAACCGTTGTACAGTTCATCCA TG-3′. This insert was digested with *Nhe*I and *Sap*I and was ligated to generate pGFP/TXB1. Plasmid vector pGFP-Met/TXB1—which contained a methionine residue insert between GFP and the intein that was reported as suitable for the production of protein-Cα-thioester [19]—was prepared using site-directed mutagenesis with the primers 5′-CTGTACAACGGTATGTGCATCACGGGA-3′ and 5′-TCCCGTGATGCACATACCGTTGTACAG-3′.

2.2 Preparation of GFP-Cα-Thioester

Fusion proteins of GFP-intein were expressed in *Escherichia coli* BL21 cells. The cell pellets (typically 2.3 g of wet cells from 500 mL of culture) were resuspended in a lysis buffer (20 mM Tris-HCl, 300 mM NaCl, pH 7.5) containing phenylmethylsulfonyl fluoride. The cells were lysed by sonication and were centrifuged. The supernatants were applied to a 5-mL-volume chitin bead column (New England Biolabs Inc.). The column was washed thoroughly in lysis buffer and rocked at 37 °C overnight in the presence of mercapto ethane sulfonic acid sodium salt (MESNa) to produce GFP-Cα-MESNa. The beads were filtered off and rinsed. Aliquots of each step were monitored using SDS-PAGE.

The solution of GFP-Cα-MESNa was concentrated 10-fold using centrifugal dialysis (Amicon Ultra-3; Millipore Corp., MA, USA). The buffer was exchanged to aqueous $NaHCO_3$ (200 mM, pH 8.5). The solution was frozen immediately until use. The procedure gave 1.0 mg of GFP product, as determined by UV absorption at 488 nm, from 500 mL culture. The band on SDS-PAGE corresponding to GFP product was subject to tryptic digestion. Following desalt and condensation with ZipTip C_{18} (Millipore Corp.), the peptides were analyzed using MALDI-TOF MS (Voyager STR; Applied Biosystems, CA, USA) using α-cyano-4-hydroxyciannamic acid as a matrix. The analysis revealed peptide fragments corresponding to 5–27, 28–42, 47–53, 81–86, 87–102, 115–127, 133–141, 142–157, and 216–240 of GFP (data not shown). The purity and molecular weight were checked using SDS-PAGE.

2.3 Synthesis of NH_2-DEG-NHCO-Chol and Cys-NH-DEG-NHCO-Chol

Cholesterol chloroformate was condensed with an excess molar amount of 4,7,10-trioxa-1,13-tridecane diamine (NH_2-DEG-NH_2). After 60 min incubation, the reaction mixture was washed with water. Then the reaction mixture was applied to a silica column and eluted. The fractions containing NH_2-DEG-NHCO-Chol were combined and evaporated. The coupling product was analyzed using TLC. FAB-MS, 633.5202 (theoretical $[M + H]^+ = 633.5206$).

In the presence of *N*,*N*-diisopropylethylamine, NH_2-DEG-NHCO-Chol was reacted with *N*-(*N*-α-trityl-*S*-trityl-L-cysteinyloxy)succinimide. After 60 min, the product was purified on a silica column. A protecting group of the product was removed through treatment with trifluoroacetic acid and triisopropylsilane. The product Cys-NH-DEG-NHCO-Chol was purified using a silica column. The fractions containing Cys-NH-DEG-NHCO-Chol were combined and evaporated. The residue was suspended in water and frozen until use. FAB-MS, 758.5122 (theoretical $[M + Na]^+ = 758.5118$).

2.4 Synthesis of F-NH-DEG-NH_2 and F-NH-DEG-NHCO-Chol

Succimidyl ester of 5-carboxyfluorescein (F) was reacted with NH_2-DEG-NH_2 or NH_2-DEG-NHCO-Chol. After 60 min of incubation, the product was purified using a silica column. After evaporation, the residue was dissolved in water. The quantity was estimated using UV measurement. FAB-MS was 579.2347 (theoretical $[M + H]^+ = 579.2343$) for F-NH-DEG-NH_2 and 1013.5507 (theoretical $[M + Na]^+ = 1013.5503$) for F-NH-DEG-NHCO-Chol, respectively.

2.5 Synthesis of Cys-Lanthanide Binding Peptide

Starting from Fmoc-Gly Wang resin, FIDTNNDGWIEGDELLLEEGG-resin was synthesized using a peptide synthesizer (ABI 433A; Applied Biosystems) with 2-(1H-benzotriazole-1-yl)-1,1,3,3-tetramethyluronium hexafluorophosphate as a coupling reagent. To this peptide resin, tBoc-Cys(Trt) was incorporated manually. Crude peptide was obtained using a cleavage reaction. It was subject to RP-HPLC purification. MALDI-TOF MS was 2440.58 (theoretical $[M + H]^+ = 2440.31$).

2.6 Native Chemical Ligation of GFP-Cα-MESNa with Cys-Derivatives

The solution of GFP-Cα-MESNa was condensed with Cys-lanthanide binding peptide, Cys-NH-DEG-NHCO-Chol, or 1,4-dithio-DL-threitol (DTT) in the presence of $NaHCO_3$, tris(hydroxypropyl)phosphine and cetyl trimethyl ammonium bromide (CTAB). The coupling mixture was incubated for 24 h at room temperature under nitrogen. The reaction buffer was exchanged to PBS repeatedly by ultracentrifugation. The GFP product concentration was determined using UV measurement. The progress of the coupling reaction was monitored using SDS-PAGE.

An aliquot of the coupling reaction mixture between GFP-Cα-MESNa and Cys-NH-DEG-NHCO-Chol was subject to chloroform–methanol protein precipitation to remove salts and detergents from the mixture. The precipitated protein was analyzed using RP-HPLC (LC10A; Shimadzu Corp., Kyoto, Japan) with a C_4 column ($5C_4$-AR300; 4.6 × 150 mm, Nacalai Tesque Inc., Kyoto, Japan). Results of MALDI-TOF MS were 26857.9 corresponding to GFP (theoretical $[M + H]^+ = 26997.9$), and 27571.1 corresponding to GFP-Chol (theoretical $[M + H]^+ = 27716.9$). A difference of 140 Da was found between the observed mass number and the calculated mass number of both unmodified and modified GFP. This result might be attributed to degradation of the first methionine residue, causing a 131 Da decrease in the mass number.

2.7 Fluorescence Microscopy

Cultured N2a cells in Opti-MEM (Invitrogen Corp. CA, USA), supplemented with 10% fetal calf serum on a glass-bottom dish, were rinsed three times with cold PBS. Each sample of modified GFP (final conc. 4.8 μM), unmodified GFP (final conc. 4.8 μM), F-NH_2 (final conc. 0.84 μM) and F-Chol (final conc. 1.2 μM) was added to the cells in cold PBS. For double staining, both modified GFP (final conc. 4.8 μM) and rhodamine-labeled 3F4 anti-prion protein antibody (final conc. ca. 1.2 μg/mL) were added to the cells in cold PBS. After 15 min incubation under a cold condition, the cells were rinsed with cold PBS. Then the cells were observed using confocal fluorescence microscopy (magnification ×60) (Fluoview FV300; Olympus Corp., Tokyo). Prion protein, a glycosyl phosphatidyl inositol-anchored protein, was used as a marker protein for the lipid raft microdomain of the cell membrane.

2.8 Density Gradient Fractionation Analysis

Density gradient fractionation analysis of the cell membrane components was performed as described by Naslavsky and colleagues [12]. Briefly, cells that had been grown confluently in two flasks (25 cm^2) were labeled with GFP-Chol or F-Chol as described above. Then the cells were lysed with 500 μL of lysis buffer (150 mM NaCl, 25 mM Tris–HCl, pH 7.5, 5 mM ETDA, 1% Triton X-100) on ice for 30 min. The lysate (400 μL) was mixed with an equal volume of ice-cold 70% Nycodenz prepared in TNE (25 mM Tris, pH 7.5, 150 mM NaCl, 5 mM EDTA) and loaded to an ultracentrifuge tube. Then the lysate was overlaid sequentially with 200 μL each of 25, 22.5, 20, 18, 15, 12, and 8% Nycodenz in TNE. The tube was spun at 200,000×g for 4 h at 4 °C using a micro-ultracentrifuge (CS 120 GX; Hitachi Ltd., Tokyo, Japan). Eleven fractions containing 200 μL each were collected from the top of the tube.

An aliquot of each fraction was subject to fluorescence analysis and immunoblotting. Fluorescence was analyzed using a microplate reader (ARVO, MX; PerkinElmer Inc., MA, USA) to detect GFP-Chol and F-Chol. For immunoblotting detection of GFP-Chol, we used mouse monoclonal anti-GFP antibody (ab1218; Abcam plc., MA, USA) as a primary antibody and rabbit anti-mouse IgG as a secondary antibody.

3 Results and Discussion

We used GFP as a model protein because of its easy traceability. Then we modified it by introducing a cholesterol (Chol) group at the C-terminal to target it to the cell

membrane of live cells. The modified GFP was produced using a combination of recombinant protein synthesis in *E. coli* and chemical synthesis.

3.1 Semi-Synthesis of GFP-Cys-NH-DEG-NHCO-Chol (GFP-Chol)

Semi-synthesis of GFP-Cys-NH-DEG-NHCO-Chol (GFP-Chol) was achieved by condensation of building blocks corresponding to GFP and Chol. The building block for GFP consisted of a GFP bearing a modification moiety. The building block for Chol consisted of Chol and a hydrophilic linker with Cys at the terminal (Fig. 1). The building block for GFP was prepared using *E. coli* recombinant protein expression; the building block for Chol was prepared using chemical synthesis. Then both building blocks were condensed using the native chemical ligation method [6] under an aqueous condition. Similar semi-synthetic strategies have been described in previous reports [5, 13–15].

The GFP-Cα-thioester was prepared by application of intein-mediated thiolysis to a GFP-intein fusion recombinant protein (Fig. 1a). To produce the recombinant protein, three constructs were examined: (1) a GFP DNA fragment was inserted into the *NheI*/*Xho*I site of pTYB1 vector (New England Biolabs Inc., MA, USA), (2) a DNA fragment was inserted into the *NheI*/*Sap*I site of pTXB1 vector (New England Biolabs Inc.), and (3) a DNA fragment of GFP plus a methionine residue between GFP and intein was inserted into the *NheI*/*Sap*I site of pTXB1 vector; the last construct was examined because methionine is reportedly a suitable amino acid residue for the production of protein-Cα-thioester [19]. Among them, the second construct—GFP DNA fragment inserted into the *NheI*/*Sap*I site of pTXB1—produced a suitable fusion recombinant protein that was then cleaved into GFP-Cα-thioester by intein-mediated thiolysis. The cleavage reaction was controlled by MESNa added to the recombinant protein solution; the GFP-Cα-thioester product was recovered as presented in Figure S10B. On the other hand, the first construct produced a recombinant protein from which no cleavage product was obtained. The third construct produced a recombinant protein that was cleaved into products having no Cα-thioester, even in the absence of MESNa and even at 4 °C.

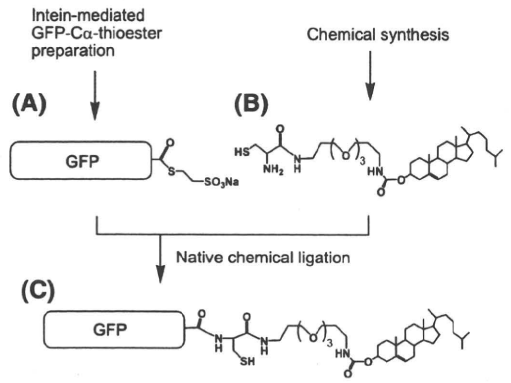

Fig. 1 Schematic representation of semisynthesis of cholesterol-modified GFP. **a** GFP-Cα-thioester preparation by intein-mediated thiolysis. **b** Synthetic scheme of the amphitropic part. The Cys residue was incorporated for the subsequent condensation reaction. Intermediates were used for the synthesis of control compounds. **c** Modification by the native chemical ligation method. The thiol exchange reaction was followed by an S–N acyl shift to generate a peptide bond

The building block for Chol (Fig. 1b) was synthesized with Chol, a hydrophilic diethylene glycol-based diamine linker (NH_2-DEG-NH_2), and a chemoselective reaction moiety to the Cα-thioester, Cys [6]. These three chemical components were condensed sequentially. Briefly, NH_2-DEG-NH_2 was reacted with Chol chloroformate. After NH_2-DEG-NHCO-Chol was isolated using a silica column, a Cys residue was incorporated at the other amino group. After deprotection and isolation, Cys-NH-DEG-NHCO-Chol was obtained. These coupling reactions and products were confirmed using TLC and FAB-MS.

The building blocks for GFP and Chol were condensed using the native chemical ligation method. The ligation reaction was performed in the presence of 20 mM of CTAB to solubilize the amphitropic unit of the building block for Chol during the ligation [7]. The product from the reaction of GFP-Cα-thioester with Cys-NH-DEG-NHCO-Chol showed no obvious mobility difference on SDS–PAGE from that of the reaction of GFP-Cα-thioester with DTT (Fig. 2, lanes 2 and 4). Therefore, we tested whether the ligation conditions and GFP-Cα-thioester were suitable for reaction by monitoring the ligation of GFP-Cα-thioester with the Cys-lanthanide binding peptide composed of 21 amino acid residues [8] (Fig. 2, lane 3). The product of this ligation showed a mobility shift. Its yield was estimated as approximately 50% of the initial material on SDS-PAGE. Therefore, we presumed that the ligation conditions and GFP-Cα-thioester were suitable for the reaction.

After both the detergent and the Cys-NH-DEG-NHCO-Chol were removed using chloroform–methanol precipitation, the ligation product was separated from unligated GFP-Cα-thioester by RP-HPLC column (Fig. 3a). In the elution profile, a peak corresponding to GFP-Cα-thioester [RT 26 min (*) in Fig. 3a] was followed by a new peak [RT 36 min (**) in Fig. 3a], indicating that the hydrophobicity of the ligation product was increased significantly. The yield of the ligation product was estimated as 45% of the initial material and was almost comparable to that of the ligation product with the Cys-lanthanide

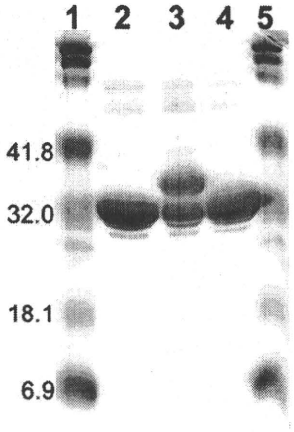

Fig. 2 Coupling reaction of GFP-Cα-thioester with Cys-derivatives. Coomassie-stained SDS-PAGE of the products from GFP-Cα-thioester reacted with DTT (*lane 2*), Cys-lanthanide binding peptide (*lane 3*) and Cys-NH-DEG-NHCO-Chol (*lane 4*) is shown. The molecular weight marker (kDa units) is included in *lanes 1* and *5*. The coupling reaction proceeded successfully in *lane 3*. No significant mobility change was observed in *lane 2* or *4*

binding peptide. Subsequent MALDI-TOF MS analysis of the material from each peak revealed that the ligation product was GFP-Chol. The mass number difference between the materials at each peak was 713 Da (Fig. 3b), which was almost identical to the calculated value of 719 Da. These results indicated that the semisynthesis was successfully performed.

3.2 Synthesis of Fluorescein-NH-DEG-NHCO-Chol (F-Chol)

Fluorescein-labeled Chol (F-Chol) was prepared by condensing fluorescein and NH_2-DEG-NHCO-Chol. Actually, F-Chol acted as a control to evaluate the Chol function. The ligation product was water-soluble and separated as described for GFP-Chol. The separation method did not affect the fluorescence function of F-Chol. Sato and colleagues reported the synthesis and application of a fluorescein ester of polyethylene glycol-modified cholesterol which labeled cholesterol-rich membranes in both live cells and in model membranes [17]. Compared to their compound, F-Chol is simpler and more stoichiometrically homogeneous. The orientation of Chol within the plasma membrane may differ dramatically according to the modification site in Chol scaffold [18]. Hedgehog proteins are modified by an ester formation between the C-terminal of the protein and the secondary alcohol of Chol [10]. Taking these into account, we decided to use the secondary alcohol group in Chol as the ligation site in the present study.

3.3 Application to Mouse Neuroblastoma N2a Cells

The GFP-Chol separation method described above, which included two protein denaturing steps, caused such denaturation of GFP-Chol that no attempt was able to refold it to an active fluorescence form. Therefore, the reaction mixture containing both GFP-Chol and GFP was used for

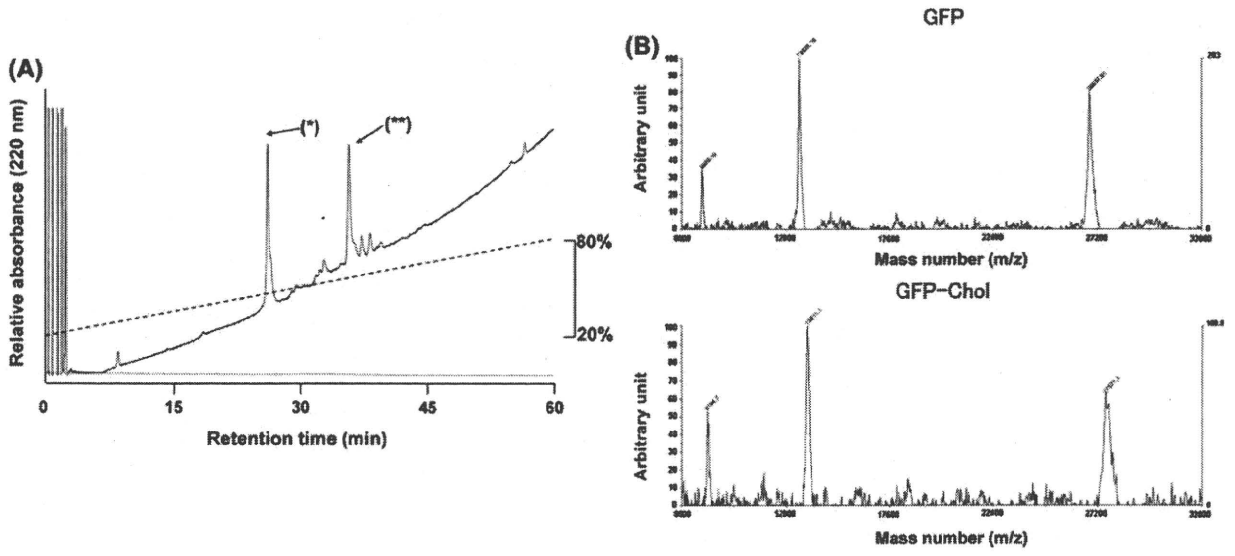

Fig. 3 Analysis of coupling reaction products. **a** RP-HPLC profile of the crude mixture after coupling reaction. The peaks *arrowed* by (*) and (**), respectively correspond to GFP and GFP-Chol. **b** MALDI-TOF MS data for GFP and GFP-Chol. Observed mass numbers for GFP and GFP-Chol were 26857.9 (theoretical $[M + H]^+ = 26997.9$) and 27571.1 (theoretical $[M + H]^+ = 27716.9$), respectively, indicating a 713 increase in mass number after Chol-modification

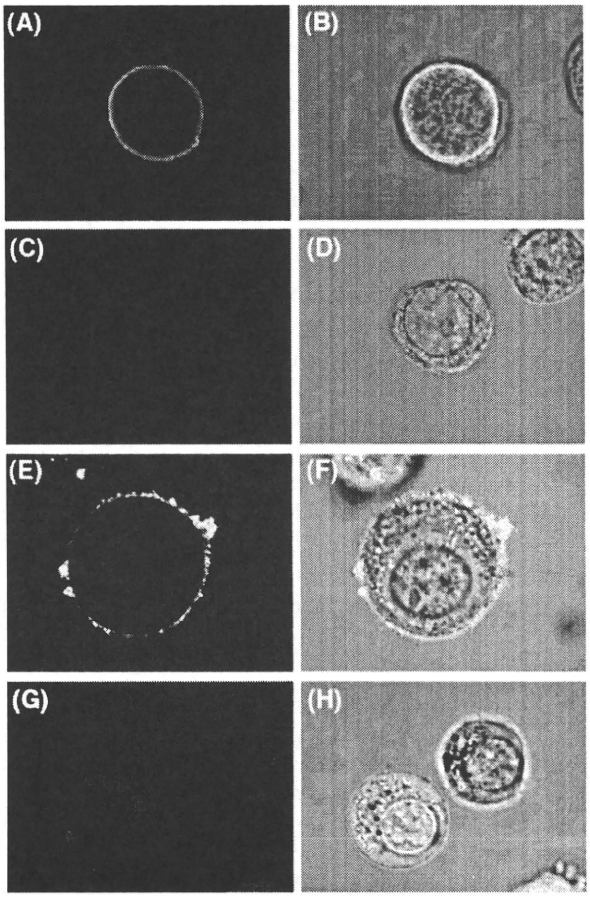

Fig. 4 Fluorescence microscopy images of GFP-Chol and control compounds in N2a cells. N2a cells were observed by confocal laser fluorescence microscopy after incubation with GFP-Chol (**a** and **b**), GFP (**c** and **d**), F-Chol (**e** and **f**) and F-NH_2 (**g** and **h**). Fluorescence images (**a**, **c**, **e** and **g**) were merged with corresponding differential interference contrast images (**b**, **d**, **f** and **h**). Fluorescence signals were observed at the cell membrane in GFP-Chol and F-Chol, but not in GFP and F-NH_2

application to live cells after extensive ultrafiltration with PBS to remove detergents. The results of this mixture sample were then compared to those of the sample containing GFP alone. The content of GFP-Chol in the mixture sample was estimated as 45% by RP-HPLC analysis (Fig. 3a). No significant difference in the fluorescence spectra were observed between the two samples (Figure S11). The GFP moiety concentration was determined by absorption at 488 nm wavelength.

The mouse neuroblastoma N2a cells were incubated with the samples at 4 °C for 15 min. Confocal fluorescent microscopy analysis revealed that the GFP-Chol was retained homogenously at the cell membrane (Fig. 4a, b), although GFP prepared by hydrolysis of GFP-Cα-thioester was rinsed off with cold PBS (Fig. 4c, d). The homogenous retention of GFP-Chol at the cell membrane was observed

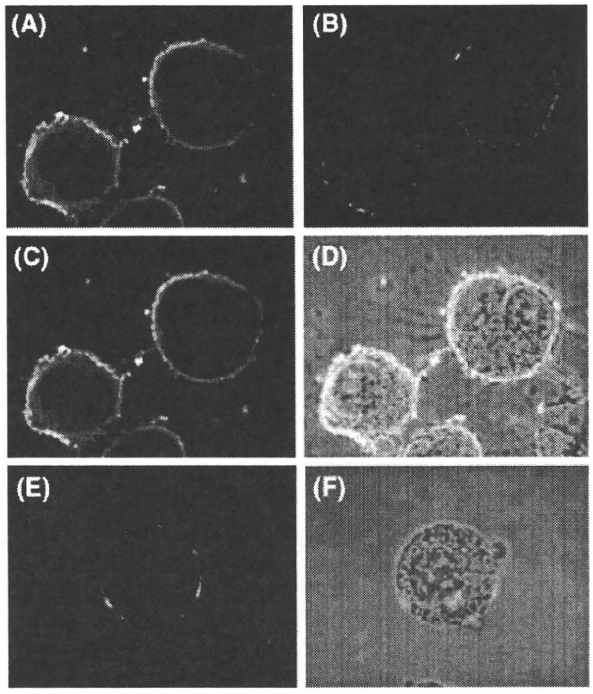

Fig. 5 Fluorescence microscopy images for GFP-Chol and prion protein in N2a cells. N2a cells were observed by confocal laser fluorescence microscopy after incubation with GFP-Chol and rhodamine-labeled anti-prion protein antibody. Fluorescence image for GFP-Chol (**a**) and for prion protein (**b**) were merged without the differential interference contrast image (**c**) or with the contrast image (**d**). The signals for GFP-Chol were rather homogenously distributed at the cell membrane as demonstrated in Fig. 4a, but those for prion protein were distributed in a patchy pattern at the cell membrane. This prion protein distribution pattern at the cell membrane was similarly observed in the cells incubated with only rhodamine-labeled anti-prion protein antibody (**e** and **f**)

also in live cells of other types, such as mouse bone marrow-derived mast cells (data not shown).

To clarify the function of Chol itself, F-Chol and F-NH_2 were also applied to the N2a cells. In fact, F-Chol was observed at the cell membrane (Fig. 4e, f). However, most of F-NH_2 was rinsed off, and a small portion was observed inside of the cells (Fig. 4g, h). The internalization of F-NH_2 might have been caused by the passive intake of an amino moiety [9], which was included in F-NH_2 but not in F-Chol. These findings suggest that Chol modification allows molecules to be targeted to the cell membrane.

To compare the distribution of GFP-Chol with that of a lipid raft marker protein in the N2a cells, we performed double staining for GFP-Chol and prion protein, a glycosyl phosphatidyl inositol-anchored protein known to localize in the lipid raft microdomain of the cell membrane [12, 20]. The signals for GFP-Chol were rather homogenously distributed at the cell membrane (Fig. 5a) as already shown in Fig. 4a. However, the signals for prion protein were distributed in a patchy pattern at the cell membrane (Fig. 5b)

and did not necessarily co-localize with the signals for GFP-Chol (Fig. 5c, d). We confirmed that the GFP-Chol treatment of the cells did not affect the distribution pattern of prion protein at the cell membrane, by comparing the prion protein images of GFP-Chol-treated N2a cells (Fig. 5b) with those of untreated N2a cells (Fig. 5e, f).

3.4 Distribution of GFP-Chol and F-Chol at the Cell Membrane

To investigate the distribution of GFP-Chol and F-Chol at the cell membrane of N2a cells, density gradient fractionation of the cell membrane components [2] was performed. Each fraction was analyzed using detection of fluorescence (Fig. 6a). We detected both GFP-Chol and F-Chol in the high-density fractions of the cell membrane. Immunoblot analysis of GFP from an aliquot of each fraction confirmed the results of the fluorescence analysis (Fig. 6b). In contrast to GFP-Chol and F-Chol, prion protein is known to distribute in the low-density fractions of the cell membrane in N2a cells [12], as demonstrated in Figure S13.

The results of either confocal laser fluorescent microscopy analysis or density gradient fractionation analysis are apparently different from those of previous studies, where proteins fused with a signal peptide for post-translational lipid-modification were expressed in the lipid raft microdomain [10, 16, 21], or where an exogenously added Chol-modified fluorescein was observed in the lipid raft microdomain [17]. This difference might be caused by our method of Chol-modification, because modified Chol may have different orientations from that of native Chol within the plasma membrane [18]. Also, it is presumable that the difference might be attributable to variations in such materials used in the experiments as cell types, modified protein types, and stoichiometry of Chol in tested molecules. In addition, it is conceivable that exposure of relatively high concentrations of our Chol-modified molecules to live cells might alter selective incorporation of the molecules into proper portions of the cell membrane or might disturb the cell membrane integrity. However, all these possibilities remain to be further evaluated.

In conventional chemical modifications of proteins, chemical reactions tend to occur more efficiently on the protein surface, where epitopes or functional groups of the proteins can be damaged. Therefore, proteins must be modified in such a fashion that their functional groups can be maintained properly. The present study demonstrated a specific chemical modification of a model protein to deliver it to the cell membrane of live cells without damaging the protein's functional activity. This kind of specific chemical modification of proteins is a key requirement for applying the proteins in in vivo or ex-vivo systems.

4 Conclusion

We demonstrated the semisynthesis of GFP specifically modified with Chol at the C-terminal. Results show that the

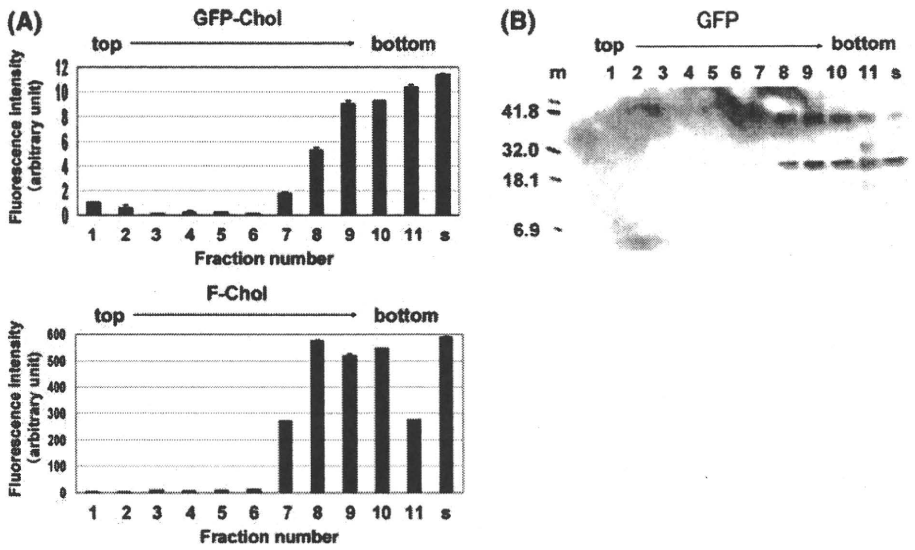

Fig. 6 Density gradient fractionation data of GFP-Chol and F-Chol in N2a cells. N2a cells incubated with GFP-Chol or F-Chol were lysed under a mild condition. The lysate was fractionated. Numbering order is from the top fraction (low density) to the bottom fraction (high density) in an 8–35% linear density gradient. The starting material before fractionation is indicated as "s". **a** Fluorescence data for GFP-Chol and F-Chol. Both fluorescence signals were distributed in higher density fractions. **b** Immunoblotting data for GFP. Signal distribution pattern for GFP was consistent with that of GFP-Chol fluorescence. The molecular weight marker in the left "m" is shown in kDa units

protein remained functional and was localized at the cell membrane, when added to live cells exogenously. These findings suggest that modifying proteins with Chol at the C-terminal is useful for targeting proteins to the cell membrane of live cells.

Acknowledgments This research was supported by Grants-in-Aid for Scientific Research No. 16750138 and No. 18750139 from the Ministry of Education, Culture, Sports, Science and Technology, Japan and by a grant from the Ministry of Health, Labour, and Welfare. MALDI-TOF MS data were obtained with the support of Biomedical Research Core of Tohoku University Graduate School of Medicine. The FAB-MS data used in this study were obtained with the assistance of Prof. Akaji, Kyoto Prefecture Medical University. This work was partly performed under the Cooperative Research Program of Institute for Protein Research, Osaka University.

References

1. Aimoto S (2001) Curr Org Chem 5:45–87
2. Brown DA, Rose JK (1992) Cell 68:533–544
3. Chong S, Shao Y, Paulus H, Benner J, Perler FB, Xu MQ (1996) J Biol Chem 271:22159–22168
4. David R, Richter MP, Beck-Sickinger AG (2004) Eur J Biochem 271:663–677
5. Dawson PE, Kent SB (2000) Annu Rev Biochem 69:923–960
6. Dawson PE, Muir TW, Clark-Lewis I, Kent SB (1994) Science 266:776–779
7. Durek T, Alexandrov K, Goody RS, Hildebrand A, Heinemann I, Waldmann H (2004) J Am Chem Soc 126:16368–16378
8. Franz KJ, Nitz M, Imperiali B (2003) Chembiochem 4:265–271
9. Guy-Caffey JK, Bodepudi V, Bishop JS, Jayaraman K, Chaudhary N (1995) J Biol Chem 270:31391–31396
10. Jeong J, McMahon AP (2002) J Clin Invest 110:591–596
11. Muir TW, Sondhi D, Cole PA (1998) Proc Natl Acad Sci USA 95:6705–6710
12. Naslavsky N, Stein R, Yanai A, Friedlander G, Taraboulos A (1997) J Biol Chem 272:6324–6331
13. Olschewski D, Seidel R, Miesbauer M, Rambold AS, Oesterhelt D, Winklhofer KF, Tatzelt J, Engelhard M, Becker CF (2007) Chem Biol 14:994–1006
14. Paulick MG, Wise AR, Forstner MB, Groves JT, Bertozzi CR (2007) J Am Chem Soc 129:11543–11550
15. Pellois JP, Muir TW (2005) Angew Chem Int Ed Engl 44:5713–5717
16. Rietveld A, Neutz S, Simons K, Eaton S (1999) J Biol Chem 274:12049–12054
17. Sato SB, Ishii K, Makino A, Iwabuchi K, Yamaji-Hasegawa A, Senoh Y, Nagaoka I, Sakuraba H, Kobayashi T (2004) J Biol Chem 279:23790–23796
18. Scheidt HA, Muller P, Herrmann A, Huster D (2003) J Biol Chem 278:45563–45569
19. Southworth MW, Amaya K, Evans TC, Xu MQ, Perler FB (1999) Biotechniques 116:118–120
20. Stahl N, Borchelt DR, Hsiao K, Prusiner SB (1987) Cell 51:229–240
21. Vincent S, Thomas A, Brasher B, Benson JD (2003) Nat Biotechnol 8:936–940